Band-structure anomalies of the chalcopyrite semiconductors $CuGaX_2$ versus $AgGaX_2$ (X=S and Se) and their alloys

Shiyou Chen and X. G. Gong
Surface Science Laboratory (National Key) and Physics Department, Fudan University, Shanghai 200433, China

Su-Huai Wei
National Renewable Energy Laboratory, Golden, Colorado 80401, USA

(Received 15 February 2007; published 31 May 2007)

We have performed systematic first-principles calculations for the structural and electronic properties of chalcopyrite semiconductors $AgGaS_2$, $AgGaSe_2$, $CuGaS_2$, $CuGaSe_2$, and their alloys. We show that, in contrast to conventional semiconductors, the band structures of these compounds exhibit several anomalous behaviors: (i) The band gaps of $AgGaX_2$ are larger than the corresponding $CuGaX_2$ (X=S and Se) compounds, despite the lattice constants of $AgGaX_2$ being much larger than for $CuGaX_2$. (ii) The valence band offsets between common-anion pairs $CuGaX_2/AgGaX_2$ are large and negative (i.e., $CuGaX_2$ has higher valence band maximum than $AgGaX_2$), opposite to their II-VI analogs. (iii) The valence band offsets between M^IGaS_2/M^IGaSe_2 (M^I=Cu, Ag) are significantly smaller than their II-VI analogs. (iv) The band gap bowing parameters for the common-anion alloys are larger than the common-cation alloys, following the same trend as the valence band offsets. Moreover, we find that the wave function localization of the conduction band minimum states at the group III site plays an important role on the band gap reduction of the chalcopyrites relative to their binary analogs. The origin of the band structure anomalies observed in this system is explained in terms of the atomic sizes and chemical potentials and the increased structural and chemical freedom of these ternary compounds.

DOI: 10.1103/PhysRevB.75.205209 PACS number(s): 71.20.Nr, 71.23.−k, 71.55.Gs, 73.61.Le

I. INTRODUCTION

The I-III-VI_2 ternary compounds are isoelectronic with the zinc-blende II-VI semiconductors.[1] For example, $CuGaX_2$ (X=S and Se) are the ternary analogs of the binary compounds ZnX, and $AgGaX_2$ are the ternary analogs of the pseudobinary compounds $Cd_{0.5}Zn_{0.5}X$. These I-III-VI_2 ternary compounds have two types of cations and crystallize in the tetragonal chalcopyrite structure, which could be considered as a (2,2) zinc-blende superlattice along the ⟨201⟩ direction. Considerable interest has been shown in these chalcopyrite compounds and their alloys due to their important technological applications in nonlinear optics, light-emitting diodes, and solar cells.[1–5] Recently, the $(Cu,Ag)GaX_2$ alloy system has attracted much attention, because these materials have direct band gaps between 1.68 and 2.65 eV, which is in the range desirable for applications in solid state lighting[6] and high-efficiency tandem solar cells.[7] $AgGaSe_2$ in the epitaxially stabilized CuAu phase is also proposed as a high-efficiency spin-polarized electron source due to its relatively large spin-orbit (SO) and crystal field (CF) splittings.[8,9] Furthermore, due to the added chemical and structural freedom of these compounds relative to their II-VI analogs, the $(Cu,Ag)GaX_2$ system exhibits some abnormal chemical trends. For example, these chalcopyrite compounds not only have large downward shifts in the band gap relative to their binary analogs, but the band gaps of $AgGaX_2$ (2.65 and 1.81 eV for X=S and Se)[10] are also larger than the corresponding $CuGaX_2$ (2.43 and 1.68 eV for X=S and Se),[10] despite that the lattice constants of $AgGaX_2$ are larger than for $CuGaX_2$. This is quite surprising because for all common-anion binary semiconductors and most of the chalcopyrites, when the cation atomic size increases, the band gap always decreases. For example, the band gap of CdS at 2.6 eV is significantly smaller than the band gap of ZnS at 3.8 eV.[10] The band gap of $CuInSe_2$ at 1.04 eV is also smaller than $CuGaSe_2$ at 1.68 eV.[10] This unusual behavior also suggests that when $Ag_xCu_{1-x}GaX_2$ alloys are formed, the band gap of the alloy can decrease together with the lattice constant, which can have important implications for the band gap engineering of lattice-matched superlattice devices.[7,11] However, the origin of these unusual behaviors for the $(Cu,Ag)GaX_2$ system has not been fully discussed. It is unclear how much of the band gap reduction relative to the binary analog is due to the change in the valence band maximum (VBM) or conduction band minimum (CBM). It is also unclear quantitatively how the band gap varies as a function of the alloy concentration x. The simple phenomenological model of Tinoco *et al.*[12] suggested that the optical bowing coefficients for $Ag_xCu_{1-x}GaX_2$ should be small because Cu and Ag have similar electronegativities. However, previous experimental studies[13,14] have shown that $Ag_xCu_{1-x}GaX_2$ alloys may have large optical bowing, especially for the sulphide alloys.

To understand the band structure anomaly in this chalcopyrite system, we have systematically performed first-principles band structure and total energy calculations for $AgGaS_2$, $AgGaSe_2$, $CuGaS_2$, $CuGaSe_2$, and their common-anion and common-cation alloys. Our calculated equilibrium structural parameters and bulk moduli are in good agreement with experimental data. For the band structure, we find the following: (i) The band gaps of $AgGaX_2$ are larger than the corresponding band gaps of $CuGaX_2$, consistent with experimental observations. (ii) The level repulsion between the anion p and the noble metal d states plays an important role in understanding the band gap reduction of the chalcopyrites

relative to their binary analogs, consistent with previous understanding.[15–18] However, we also find that the wave function localization of the CBM states at the group III Ga site,[19] and the displacement of the anion away from the ideal zinc-blende site,[20] are important in explaining the band gap anomalies in this system. (iii) The valence band offsets between the common-anion pairs $CuGaX_2/AgGaX_2$ are large and negative (i.e., $CuGaX_2$ has higher VBM than $AgGaX_2$), opposite to their II-VI analogs where CdX has higher VBM than ZnX.[21] (iv) The valence band offsets between M^IGaS_2/M^IGaSe_2 (M^I=Cu, Ag) are smaller than their II-VI analogs. (v) The band gap bowing parameters for the common-anion alloys are larger than the common-cation alloys, following the same trend as the valence band offsets. In the following, we will describe our calculation methods and discuss the origin of the anomalies observed in this system.

II. CALCULATION METHODS

The band structure and total energy calculations are performed using the density functional theory as implemented in the plane wave VASP code.[22,23] For the exchange-correlation functional, we used the generalized gradient approximation (GGA) of Perdew and Wang, known as PW91.[24] The valence electron configurations used in our calculations are Cu($3d^{10},4s^1$), Ag($4d^{10},5s^1$), Ga($3d^{10},4s^2,4p^1$), S($3s^2,3p^4$), and Se($4s^2,4p^4$). The interaction between the core electrons and the valence electrons is included by the standard frozen-core projector augmented-wave (PAW) potentials provided within the VASP package.[25,26] An energy cutoff of 300 eV was applied in all cases. For the Brillouin zone integration, we used the k-point meshes that are equivalent to the $4\times4\times4$ Monkhorst-Pack k-point meshes[27,28] in the zinc-blende Brillouin zone.

The valence band offset $\Delta E_v(ABX_2/A'BX_2')$ is calculated following the same procedure as in the core-level photoemission measurement,[29,30] where the valence band offset is defined as

$$\Delta E_v = \Delta E^{ABX_2}_{\mathrm{VBM},C} - \Delta E^{A'BX_2'}_{\mathrm{VBM}',C'} + \Delta E_{C,C'}. \quad (1)$$

Here,

$$\Delta E^{ABX_2}_{\mathrm{VBM},C} = E^{ABX_2}_{\mathrm{VBM}} - E^{ABX_2}_{C} \quad (2)$$

is the core level to valence band maximum energy separations for ABX_2 (with similar expression for $A'BX_2'$), and

$$\Delta E_{C,C'} = E^{ABX_2}_{C} - E^{A'BX_2'}_{C'} \quad (3)$$

is the difference in core level binding energy between ABX_2 and $A'BX_2'$ on each side of the interface, which can be obtained from the calculation of an $(ABX_2)_n/(A'BX_2')_n$ (001) superlattice. In our calculation, we construct a (2×2) (001) superlattice, where all the structural parameters are fully relaxed. To obtain the conduction band offsets ΔE_c, we use the relationship

$$\Delta E_c = \Delta E_g + \Delta E_v, \quad (4)$$

where ΔE_g is the measured band gap difference between ABX_2 and $A'BX_2'$.

To calculate the formation energy and optical bowing parameters of the random chalcopyrite alloys of $Ag_xCu_{1-x}GaX_2$ and $M^IGa(Se_xS_{1-x})_2$, we used the more efficient special quasirandom structures (SQS) approach.[31,32] In the SQS approach, instead of occupying the mixed-atom sites of a huge unit cell randomly to gain statistical significance, a relatively smaller unit cell is used, in which the mixed-atom sites are occupied in a way that the physically most relevant structural correlation functions $\bar{\Pi}_{k,m}$ for atomic clusters (k,m) with k vertices and up to the mth neighbor are closest to the exact values in an infinite random alloy $[\bar{\Pi}_{k,m}=(2x-1)^k]$. Because the physical properties of an alloy are uniquely determined by its atomic structure, the SQS that mimic the atomic correlation function of a random alloy should also have physical properties similar to the random alloy.

In this study, we construct SQS containing 64 atoms in the unit cell. The lattice vectors are

$$\vec{a}_1 = (2,0,0)a, \quad \vec{a}_2 = (0,2,0)a, \quad \vec{a}_3 = (0,0,2\eta)a, \quad (5)$$

where $\eta=c/2a$ and a and c are the lattice constants perpendicular and parallel to the c axis of the tetragonal chalcopyrite cell. In an ideal case, $\eta=1$. For the common-anion $Ag_xCu_{1-x}GaX_2$ alloys, there are 16 sites that are occupied by the group I Ag and Cu atoms, whereas for common-cation $M^IGa(Se_xS_{1-x})_2$ alloys, there are 32 mixed-anion sites. The occupation of these sites for the SQS at $x=0.25$ and $x=0.5$ is given in Table I, and their structural correlations function $\bar{\Pi}_{k,m}$ is given in Table II, compared with ideal random alloy correlation functions. As can be seen, the quality of the SQSs used in this calculation is reasonably good.

III. RESULTS OF THE TERNARY COMPOUNDS

A. Structural parameters and bulk moduli

The M^IGaX_2 compounds studied here crystallize in the tetragonal chalcopyrite structure (Fig. 1), with space group

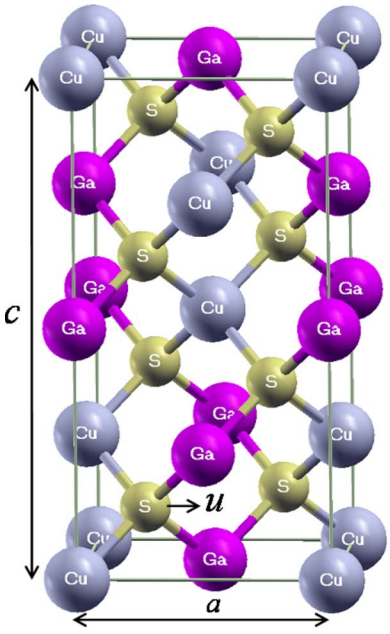

FIG. 1. (Color online). Crystal structure of chalcopyrite $CuGaS_2$.

TABLE I. Atomic coordinates and occupation of the SQS used in our calculation for mixed-cation $Ag_xCu_{1-x}GaX_2$ alloys and the mixed-anion $M^IGa(Se_xS_{1-x})_2$ alloys at concentration $x=0.25,0.5$. For clarity, only the mixed sublattice coordinates are shown. We assumed $\eta=c/2a=1$.

$Ag_xCu_{1-x}GaX_2$				$M^IGa(S_xSe_{1-x})_2$			
$x=0.25$		$x=0.5$		$x=0.25$		$x=0.5$	
Type	Coordinates	Type	Coordinates	Type	Coordinates	Type	Coordinates
Ag	1.5 1.5 1.0	Ag	0.0 0.0 0.0	S	0.25 0.75 0.75; 1.25 0.25 1.25	S	0.25 0.25 0.25; 1.25 0.25 0.25
Ag	1.0 1.5 0.5	Ag	0.0 1.0 0.0	S	0.25 1.75 0.75; 1.25 0.75 0.75	S	0.25 0.25 1.25; 1.25 0.75 1.75
Ag	0.5 1.0 1.5	Ag	1.0 1.0 0.0	S	0.75 0.25 0.75; 1.25 1.25 0.25	S	0.25 1.25 0.25; 1.25 1.75 0.75
Ag	1.5 1.0 1.5	Ag	0.5 1.5 1.0	S	0.75 0.75 0.25; 1.75 1.75 0.25	S	0.25 1.75 1.75; 1.25 1.75 1.75
Cu	0.0 0.0 0.0	Ag	0.0 0.5 0.5	Se	0.25 0.25 0.25; 1.25 0.25 0.25	S	0.75 0.25 1.75; 1.75 0.75 0.25
Cu	0.0 1.0 0.0	Ag	0.0 1.5 0.5	Se	0.25 0.25 1.25; 1.25 0.75 1.75	S	0.75 1.25 0.75; 1.75 1.25 1.75
Cu	1.0 0.0 0.0	Ag	1.0 0.5 0.5	Se	0.25 0.75 1.75; 1.25 1.25 1.25	S	0.75 1.25 1.75; 1.75 1.75 0.25
Cu	1.0 1.0 0.0	Ag	0.5 0.0 1.5	Se	0.25 1.25 0.25; 1.25 1.75 0.75	S	0.75 1.75 0.25; 1.75 1.75 1.25
Cu	0.5 0.5 1.0	Cu	1.0 0.0 0.0	Se	0.25 1.25 1.25; 1.25 1.75 1.75	Se	0.25 0.75 0.75; 1.25 0.25 1.25
Cu	0.5 1.5 1.0	Cu	0.5 0.5 1.0	Se	0.25 1.75 1.75; 1.75 0.25 0.75	Se	0.25 0.75 1.75; 1.25 0.75 0.75
Cu	1.5 0.5 1.0	Cu	1.5 0.5 1.0	Se	0.75 0.25 1.75; 1.75 0.25 1.75	Se	0.25 1.25 1.25; 1.25 1.25 0.25
Cu	0.0 0.5 0.5	Cu	1.5 1.5 1.0	Se	0.75 0.75 1.25; 1.75 0.75 0.25	Se	0.25 1.75 0.75; 1.25 1.25 1.25
Cu	0.0 1.5 0.5	Cu	1.0 1.5 0.5	Se	0.75 1.25 0.75; 1.75 0.75 1.25	Se	0.75 0.25 0.75; 1.75 0.25 0.75
Cu	1.0 0.5 0.5	Cu	0.5 1.0 1.5	Se	0.75 1.25 1.75; 1.75 1.25 0.75	Se	0.75 0.75 0.25; 1.75 0.25 1.75
Cu	0.5 0.0 1.5	Cu	1.5 0.0 1.5	Se	0.75 1.75 0.25; 1.75 1.25 1.75	Se	0.75 0.75 1.25; 1.75 0.75 1.25
Cu	1.5 0.0 1.5	Cu	1.5 1.0 1.5	Se	0.75 1.75 1.25; 1.75 1.75 1.25	Se	0.75 1.75 1.25; 1.75 1.25 0.75

$I\bar{4}2d$ (D_{2d}^{12}). This structure can be described by three structural parameters: the lattice constant a, the tetragonal ratio $\eta=c/2a$, and the anion displacement u. The u parameter is related to the two types of anion-cation bond lengths by

$$u=\frac{1}{4}+\frac{R_{M^I\text{-}X}^2-R_{\text{Ga-}X}^2}{a^2}, \tag{6}$$

where $R_{M^I\text{-}X}$ and $R_{\text{Ga-}X}$ are the bond lengths of M^I-X and Ga-X, respectively. In the ideal structure with equal M^I-X and Ga-X bond lengths, $u=0.25$. If u is larger than 0.25, anion atom X is displaced from the noble metal side toward the Ga side.

To obtain the equilibrium structural parameters, we first search at each volume the lattice vectors and atomic positions that give the minimum total energy. The calculated total energies as a function of the volume are then fitted to Murnaghan's equation of states (EOS)[33] to obtain the equilibrium volume and the corresponding lattice parameters, the bulk modulus B_0, and the pressure derivative of the bulk modulus B'. The calculated structural parameters are listed in Table III. We find that the calculated lattice constants are slightly larger than the experimental values,[1] as found in most GGA calculations. The calculated u parameters also agree well with the experimental data,[1,34] considering that accurate experimental determination of the u parameter is rather difficult. The calculated bulk moduli B_0 are systematically smaller than the experiment values. This is mostly related to the slight overestimation of the equilibrium volume in the GGA calculation. To correct this error, we have also given in Table III the calculated bulk moduli at the experimental volume (shown in parentheses) using the formula of Murnaghan's EOS

$$B(V_{exp})=B_0+B'P(V_{exp}), \tag{7}$$

where $P(V_{exp})$ is the calculated pressure at the experimental volume V_{exp}. We see that after this correction, the calculated

TABLE II. Atomic correlation functions $\bar{\Pi}_{k,m}$ of the SQS used in our calculation at concentration $x=0.25,0.5$, and compared with the ideal values $(2x-1)^k$ of the random alloy.

	$\bar{\pi}_{2,1}$	$\bar{\pi}_{2,2}$	$\bar{\pi}_{2,3}$	$\bar{\pi}_{2,4}$	$\bar{\pi}_{3,1}$	$\bar{\pi}_{3,2}$	$\bar{\pi}_{4,1}$	$\bar{\pi}_{4,2}$
				$Ag_xCu_{1-x}GaX_2$				
$x=0.25$:								
SQS	1/4	1/4	3/16	0	−1/6	0	0	0
Random	1/4	1/4	1/4	1/4	−1/8	−1/8	1/16	1/16
$x=0.5$								
SQS	0	0	−1/8	0	0	0	0	0
Random	0	0	0	0	0	0	0	0
				$M^IGa(S_xSe_{1-x})_2$				
$x=0.25$:								
SQS	1/4	1/6	11/48	1/4	−1/8	−5/48	0	1/12
Random	1/4	1/4	1/4	1/4	−1/8	−1/8	1/16	1/16
$x=0.5$:								
SQS	0	0	0	0	0	0	0	−1/12
Random	0	0	0	0	0	0	0	0

TABLE III. Calculated structural parameters a, $\eta=c/2a$, and u, the bulk moduli at theoretical and experimental volumes, the pressure derivative of bulk modulus B', the band gap E_g, and its derivative with respect to the u parameter dE_g/du, and the crystal field and spin orbital splitting Δ_{CF} and Δ_{SO} for the four $M^I GaX_2$ compounds. The calculated results are compared with available experimental data.

Structure		a (Å)	$\eta=c/2a$	u	B_0 $[B(V_{exp})]$ (GPa)	B'	E_g (eV)	dE_g/du (eV)	Δ_{CF} (eV)	Δ_{SO} (eV)
$CuGaSe_2$	Calculated	5.6704	0.993	0.2443	60.3 (74.3)	4.8	0.0291	11.49	−0.0958	0.2040
	Experimental	5.614[a]	0.982[a]	0.250[a]	76.6[b], 71[c]		1.68[d]		−0.139[d]	0.238[d]
$AgGaSe_2$	Calculated	6.0529	0.926	0.2794	50.7 (67.3)	5.02	0.2234	15.80	−0.2420	0.2475
	Experimental	5.985[e]	0.911[e]	0.272[e]	63.8[b],65±10[f]	4[f]	1.81[d]		−0.25[d]	0.30[d]
$CuGaS_2$	Calculated	5.3700	0.991	0.2491	75.1 (85.5)	4.7	0.6932	15.37	−0.1213	−0.0163
	Experimental	5.349[e]	0.979[e]	0.25[e]	95.8[b], 94[g]		2.43[d]		−0.129[d]	
$AgGaS_2$	Calculated	5.7742	0.916	0.2844	60.8 (74.3)	4.7	0.9455	18.62	−0.2596	−0.0218
	Experimental	5.755[e]	0.932[e]	0.282[e]	77.6[b],66.8[f]	4[f]	2.65[d]		−0.28[d]	

[a]Reference 34.
[b]References 35 and 36.
[c]Reference 37.
[d]Reference 10.
[e]Reference 1.
[f]Reference 38.
[g]Reference 39.

bulk moduli are in very good agreement with experimental values.

B. Band structures

Figure 2 describes schematically how the band structure of the chalcopyrites are evolved from the zinc-blende analogs.[40] For direct-gap zinc-blende semiconductors with T_d symmetry, such as for ZnS and ZnSe, VBM is a bonding triply degenerate Γ_{15} state, composed of mainly the anion p and cation d orbitals [Fig. 3(d)], whereas CBM is an antibonding Γ_1 state, composed of mainly cation s and anion s orbitals [Fig. 3(c)]. In chalcopyrites with the lower D_{2d} symmetry, the triply degenerate Γ_{15} VBM state splits into nondegenerate Γ_{4v} and doubly degenerate Γ_{5v} states.[16,40] The crystal field splitting $\Delta_{CF}=E(\Gamma_{5v})-E(\Gamma_{4v})$ is defined as positive if the Γ_{5v} states lie above the Γ_{4v} state. When the spin-orbit interactions are included, the Γ_{5v} levels split further into two levels, Γ_{6v} and Γ_{7v}, and the nondegenerate Γ_{4v} state transforms into another Γ_{7v} state. The spin-orbital splitting Δ_{SO} can be obtained by fitting the calculated energy levels to the quasicubic model of Hopefield.[41,42] For the four compounds studied here, the calculated Δ_{CF} and Δ_{SO} are also listed in Table III. We see that they are in good agreement with available experimental data. We find the following: (i) All four compounds have negative Δ_{CF}, because the $\eta=c/2a$ ratios for these compounds are less than one. The two Ag compounds have large negative Δ_{CF}, because their η ratios have larger deviation from unity. (ii) The Δ_{SO} for these chalcopyrite compounds are small compared to their II-VI analogs (~0.4 eV for selenides and 0.1 eV for sulphides). This is because the VBM in chalcopyrite compounds contains much more cation d orbital component [Fig. 3(b)] than in its II-VI analogs.

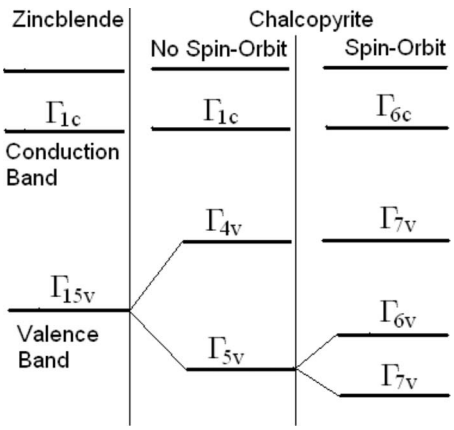

FIG. 2. Schematic plot of the band edge states at Γ for the zinc-blende and chalcopyrite compounds (see Ref. 40).

Our GGA-calculated band gaps for the four chalcopyrite compounds are also shown in Table III. We see that GGA severely underestimated the band gaps. However, the general chemical trend of the band gap variation is reproduced in the GGA calculations, i.e., the band gaps of the sulphides are larger than the selenides, and the band gaps of the Ag compounds are larger than the Cu compounds. The band gaps of the chalcopyrite compounds are also much smaller than the corresponding II-VI analogs.[10] In the past,[15,16,29,43,44] the large reduction of the band gap of the chalcopyrites relative to their II-VI analogs are mostly attributed to the larger p-d coupling in the chalcopyrites, because the group I noble metals Cu or Ag have much higher d orbital energies (Table IV), and the coupling is inversely proportional to the energy separation between the anion p and cation d energy states. This is clearly seen in Figs. 3(b) and 3(d), where the VBM of the $CuGaSe_2$ contains much more Cu d orbital character than Zn d orbital character for ZnSe. However, Fig. 3(a) also shows that the CBM of $CuGaSe_2$ is more localized on the Ga site. Because the Ga 4s orbital energy is deeper than the Zn 4s orbital energy (Table IV), this suggests that the CBM of the chalcopyrites is lower in energy than the II-VI analog,

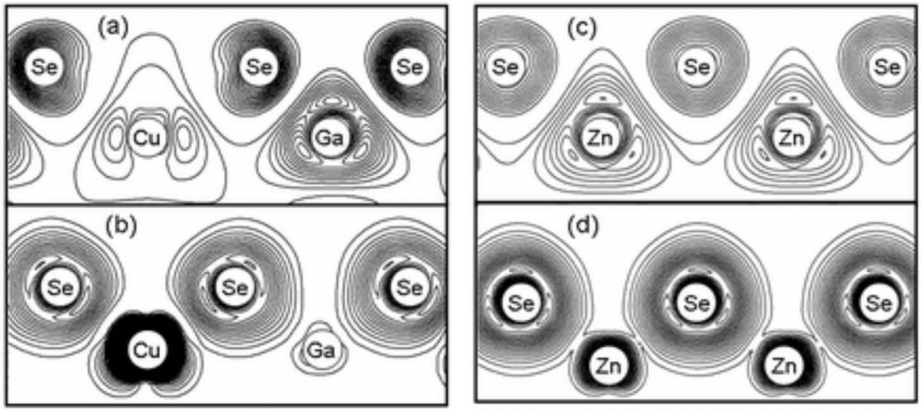

FIG. 3. Contour plot of the charge density of the CBM and VBM states of $CuGaSe_2$ and ZnSe. (a) is the CBM and (b) the VBM states of $CuGaSe_2$; (c) is the CBM and (d) the VBM of ZnSe.

thus also contributing to the band gap reduction. To study this effect more quantitatively, we have calculated the band offsets (see below) between ZnX/CuGaX_2, as shown in Fig. 4(a). We see that for X=S and Se, the CBMs of the chalcopyrites are indeed lower than their II-VI analogs and about one-quarter of the band gap reduction from II-VI to its chalcopyrite analogs is due to the lowering of the CBM.

One interesting observation from our calculations, which is consistent with experimental data, is that AgGaX_2 has a larger band gap than CuGaX_2. This is quite unusual, because AgGaX_2 has larger lattice constants than CuGaX_2 and, in common-anion binary semiconductors and other chalcopyrites, the band gap decreases when the lattice constant increases. This band gap anomaly could be explained as follows: (i) As we discussed above, the p-d level repulsion between noble metal d and anion p states pushes up the VBM, reducing the band gap. Cu has shallower d orbital energy (Table IV) and smaller atomic size, so p-d repulsion is much larger in CuGaX_2 than in AgGaX_2. Indeed, when we perform a linearized augmented plane wave (LAPW)[45] calculation and remove the cation d orbitals from the basis functions, we find that CuGaX_2 has a larger band gap than AgGaX_2. (ii) Ag is much larger than Cu. So, for AgGaX_2 the anion is pushed away from Ag toward Ga, giving a large u parameter. This anion displacement lowers the VBM because the increased M^I-X bond length reduces the p-d repulsion. This displacement also moves up the CBM, because the CBM state is more localized on the Ga site, so the reduced Ga-X bond (with respect to the ideal u=1/4 position) moves up the antibonding CBM state. To show this more quantitatively, we have calculated dE_g/du for the four compounds studied here and the results are listed in Table III. We see that dE_g/du is very large for these compounds, indicating that the band gap is very sensitive to the displacement. Indeed, if AgGaX_2 is calculated at the same u parameter as CuGaX_2, its band gap is smaller than that of CuGaX_2.

The fact that M^IGaSe$_2$ has a smaller band gap than M^IGaS$_2$ follows the common rule of the conventional semiconductors. Se has higher p orbital energy than S (Table IV), so the VBM in selenides is higher than in sulfides, although the stronger p-d hybridization in sulfides reduces the difference.[29] Se also has a lower s orbital energy level (Table IV) and larger atomic size, so the antibonding CBM state has a lower energy in selenides. Therefore, as a whole, the band gap of selenide is smaller than the corresponding sulphide.

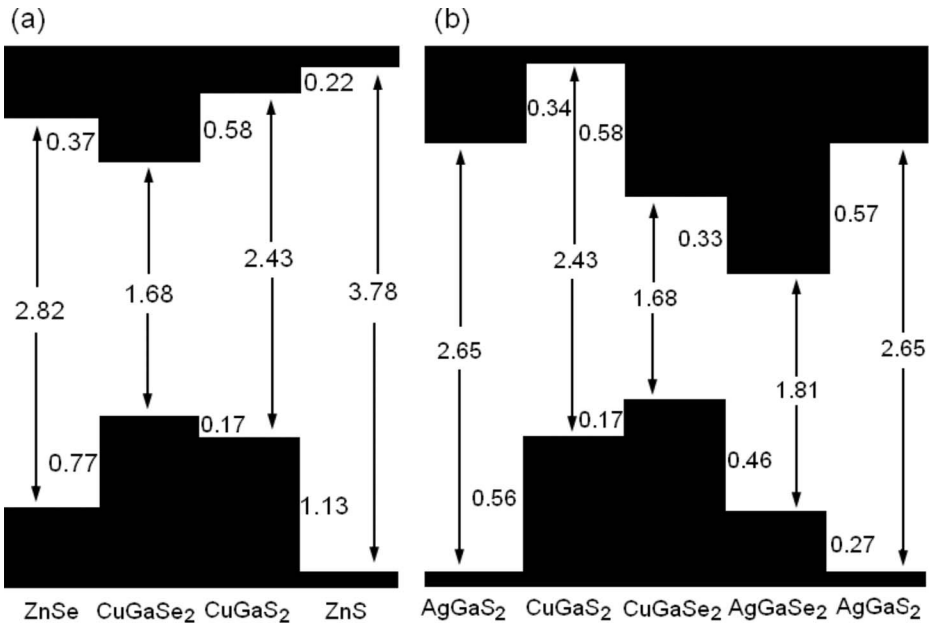

FIG. 4. Calculated valence and conduction band offsets for (a) between ZnX and CuGaX_2 (X=S, Se) and (b) between M^IGaX_2 (M^I=Cu, Ag, X=S, Se).

TABLE IV. Calculated atomic valence orbital energies ϵ_s, ϵ_p, and ϵ_d (in eV) of related elements. The calculations are performed using local density approximation within the density functional theory.

Atom	ϵ_s	ϵ_p	ϵ_d
Cu	−4.95		−5.39
Ag	−4.80		−7.73
Zn	−6.31	−1.31	−10.49
Cd	−6.04	−1.41	−11.96
Ga	−9.25	−2.82	−19.18
In	−8.55	−2.78	−18.75
S	−17.36	−7.19	
Se	−17.56	−6.74	−53.45

C. Band offsets

The above analysis can be seen more clearly and quantitatively from the calculated band offsets between $M^I GaX_2$ (M^I=Cu and Ag, X=S and Se) using the method described in Sec. II. The results are shown in Fig. 4.

For common-anion chalcopyrites, $CuGaX_2/AgGaX_2$, the band alignment is "type II," that is, the VBM is higher on the Cu compound side and the CBM is lower on the Ag compound side. The valence band offset is unusually large and *negative*, indicating that in this chalcopyrite system, the valence band offsets not only do not obey the common-anion rule, which states that the valence band offset for the common-anion system should be small, they also have an opposite sign compared to their II-VI analogs. This is because in most conventional common-anion semiconductors, the VBM is mainly a p-p bonding state. Because the cation p orbital energies are similar for atoms in the same column (Table IV), the bonding VBM state of the one with a smaller lattice constant is pushed down more than the large lattice constant one, so the VBM of the small lattice constant is usually slightly lower.[30] However, for the chalcopyrite system studied here, the VBM has large antibonding p-d characters, which push the VBM up.[30] As discussed above, the p-d coupling in Cu compounds is much stronger than Ag compounds, caused partly by the smaller p-d energy difference and partly by the smaller bond length, so the VBM of the Cu compounds are pushed up more than the Ag compounds. This explains why Cu compounds have higher VBM than the corresponding Ag compounds. On the other hand, the CBMs of the Ag compounds are lower because Ag has a larger atomic size than Cu, which reduces the s-s level repulsion between Ag and anions.[30] It is interesting to note that for mixed group III common-anion chalcopyrites, such as $CuAlSe_2$, $CuGaSe_2$, and $CuInSe_2$, previous calculation[29] showed that of their valence band offsets follow closely the common-anion rule and the band alignment is type I.

For the common-cation pairs, the M^IGaS_2/M^IGaSe_2 alignment is type I. The valence band offset reflects the large difference between anion p orbital energies of sulphur and selenium (Table IV). However, because the sulfides with low p orbital energy also have larger p-d repulsion, the difference between the p orbital energy in this chalcopyrite system is reduced compared to its II-VI analogs.[29,30] Moreover, because the Cu compounds have larger p-d coupling, the VBM offset in the Cu pairs (0.17 eV) is smaller than in the Ag pairs (0.27 eV). Because the Ga-Se bond length is also larger than the Ga-S bond length, the antibonding CBM state is lower on the selenide side.

IV. RESULTS OF CHALCOPYRITE ALLOYS

Early experimental studies and theoretical calculations show that many physical properties P of semiconductor alloy A_xB_{1-x} as a function of x follow the quadratic rules as follows:

$$P(x) = xP(A) + (1-x)P(B) - b_P x(1-x), \tag{8}$$

where b_P is the so-called bowing parameter. In the following, we will calculate the bowing parameters for the lattice constants, anion-cation bond lengths, band gaps, and the formation energies.

A. Lattice constant and bond lengths

Our calculated results show that the lattice constants of the alloy obey Vegard's rule,[46] i.e., the lattice constant bowing parameter b_a is zero, or

$$a(x) = xa(A) + (1-x)a(B). \tag{9}$$

The anion-cation bond lengths averaged over a given type also follow a linear relationship, but their variation as a function of x is much smaller than the variation in lattice constants, i.e., they have nearly the same values as in pure constituents. For example, in $Ag_xCu_{1-x}GaS_2$ alloys, Ag-S and Cu-S bond lengths are distinct and close to their ideal values in their ternary $AgGaS_2$ and $CuGaS_2$ compounds, respectively. The anion-cation bond lengths as functions of x for the four alloys are plotted in Fig. 5. We can see clearly that the deviation from the ideal values is within 0.1 Å for all bonds. The conservation of the bond lengths in these chalcopyrite alloys indicates that the ratio of bond-bending over bond-stretching force[47,48] is small for this system.

Some interesting trends of the small bond length variations can also be identified in Fig. 5. In mixed group I $Ag_xCu_{1-x}GaX_2$ alloys, the common Ga-X bond length is almost unchanged with concentration x, whereas the Ag-X and Cu-X bond lengths associated with the mixed group I elements increase with x. This is consistent with the fact that the Ga-X bond lengths are nearly identical in $CuGaX_2$ and $AgGaX_2$, because the local environment surrounding Ga is not changed with the alloy concentration x. In common-cation $M^IGa(Se_xS_{1-x})_2$ alloys, Ga-S and Ga-Se bonds elongate with increasing selenium concentration x, while the bond lengths between the noble metal M^I and anions has a much smaller increase with x. This is because the M^I-X bond is more ionic than the Ga-X bond, i.e., it has a smaller ratio of bond-bending over bond-stretching force than the Ga-X bond,[47,48] so its bond lengths are conserved better than the Ga-X bonds.

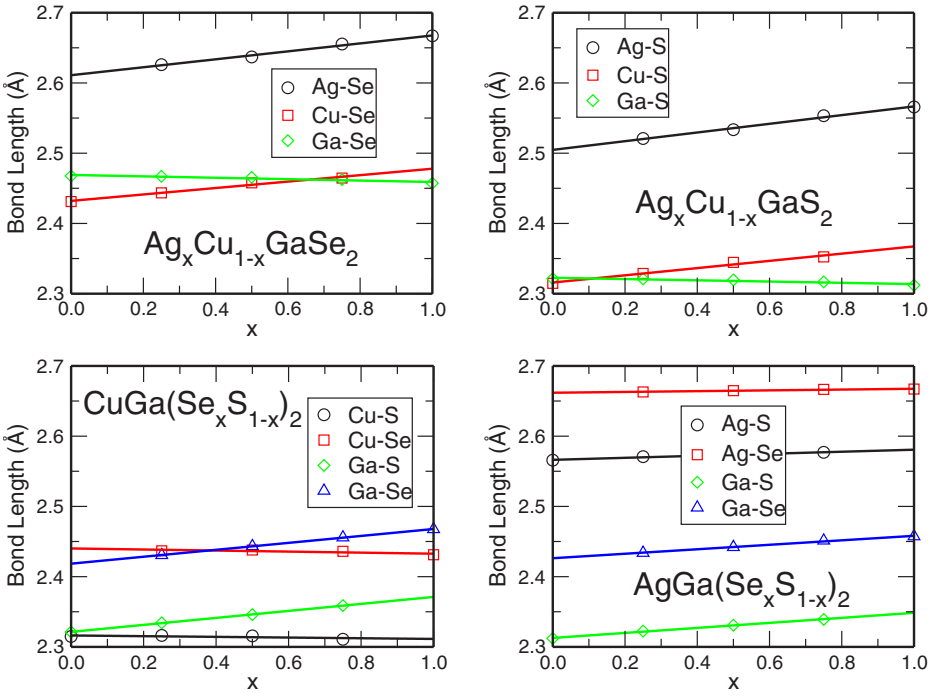

FIG. 5. (Color online). The calculated bond lengths averaged over each type for $Ag_xCu_{1-x}GaX_2$ and $M^IGa(Se_xS_{1-x})_2$ alloys at $x=0$, 0.25, 0.5, 0.75, and 1. The lines are guide for the eye only.

B. Optical bowing parameters

Due to the level repulsion between chalcopyrite energy levels in the alloy, the band gap of the alloy has a downward shift from the linear average, which can be described as

$$E_g(A_xB_{1-x}) = xE_g(A) + (1-x)E_g(B) - b_gx(1-x), \quad (10)$$

where E_g is the band gap, and b_g is the band gap (optical) bowing parameter. Note that because the bowing parameters are obtained using the band gap difference, the GGA band gap errors are largely canceled in the calculation.

The electronic band gaps of $Ag_xCu_{1-x}GaX_2$ and $M^IGa(Se_xS_{1-x})_2$ at $x=0.25$, 0.5, and 0.75 are calculated using the SQS approach as described in Sec. II. We find that all these alloys have direct band gaps. Together with the calculated band gap values of pure ternary compounds, the bowing parameter b_g can be calculated at different x according to Eq. (10). In Fig. 6, we plot the GGA-corrected band gaps of the alloys as functions of the alloy concentration x. Here, we assume that the GGA band gap error is linear with concentration x. The calculated results are then fitted to Eq. (10) to get a global bowing parameter also shown in Fig. 6. Experi-

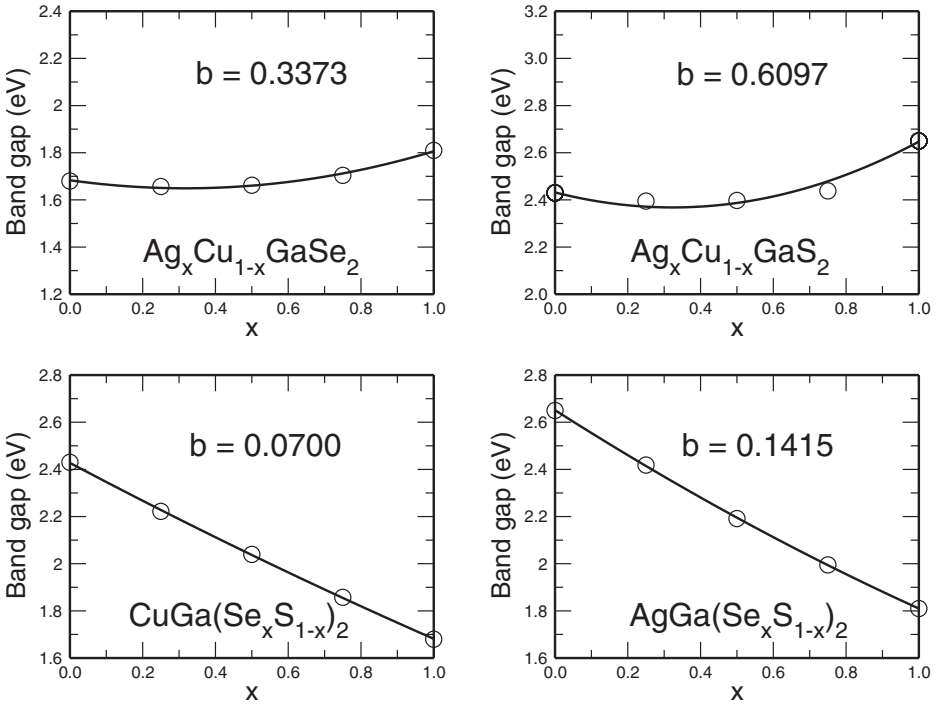

FIG. 6. The band gap of $Ag_xCu_{1-x}GaX_2$ and $M^IGa(Se_xS_{1-x})_2$ alloys at composition $x=0$, 0.25, 0.5, 0.75, and 1. A fitting curve according to Eq. (10) is also given with the optical bowing parameters b (in eV) shown in the figure.

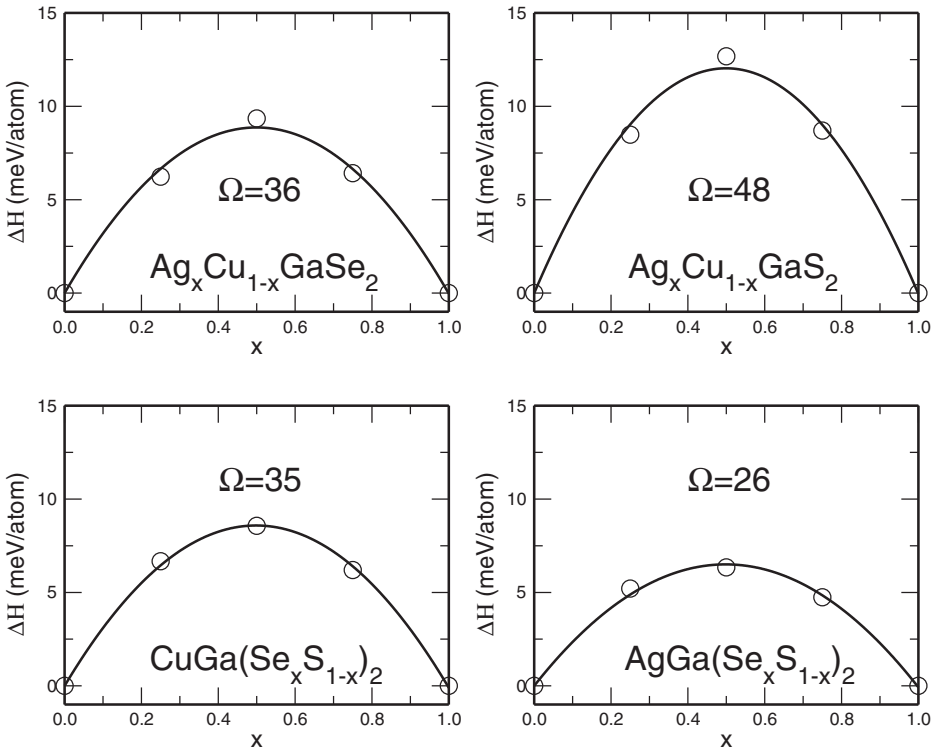

FIG. 7. Mixing enthalpies of $Ag_xCu_{1-x}GaX_2$ and $M^IGa(Se_xS_{1-x})_2$ alloys at composition $x=0.25, 0.5, 0.75$. The fitting curves according to Eq. (10) are also given with the interaction parameters Ω (in meV/atom).

mental values of the bowing parameters are ~0.79 eV for $Ag_xCu_{1-x}GaS_2$,[13] ~0.28 eV for $Ag_xCu_{1-x}GaSe_2$,[14] and ~0 eV for $CuGa(Se_xS_{1-x})_2$.[49] Our results are in good agreement with these available experimental values. Moreover, we find that the bowing parameters of mixed-cation $Ag_xCu_{1-x}GaX_2$ alloys are significantly larger than those of mixed-anion $M^IGa(Se_xS_{1-x})_2$ alloys.

In semiconductor alloys, the optical bowing parameter is usually large if the pure compounds have a large chemical and size difference.[29] The chemical and size difference can be reflected by the valence and conduction band offsets. From Fig. 4 and Table III, we can see clearly that mixed-cation alloys $Ag_xCu_{1-x}GaX_2$ have larger valence band offset and larger lattice mismatch than mixed-anion alloys, so the optical bowing parameters of mixed-cation alloys are significantly larger. Note that, unlike the chalcopyrite alloys, the mixed anion binary analog $ZnSe_xS_{1-x}$ has a large optical bowing parameter (0.50 eV) because the band offset in ZnS/ZnSe (0.53 eV) is large due to reduced *p-d* coupling.[29]

C. Mixing enthalpies

The alloy mixing enthalpy is defined as

$$\Delta H(x) = E_{tot}(A_xB_{1-x}) - xE_{tot}(A) - (1-x)E_{tot}(B), \quad (11)$$

where $E_{tot}(A)$ and $E_{tot}(B)$ are the total energy of pure A and B. For the alloys studied in this paper, we find the bowing parameter [Eq. (8)] for the mixing enthalpy is nearly a constant, i.e.,

$$\Delta H(x) = \Omega x(1-x), \quad (12)$$

where $\Omega = b_E$ is the so-called interaction parameter.

Figure 7 gives our calculated mixing enthalpies ΔH for the alloys at different concentrations $x=0.25$, 0.5, 0.75. The fitted curves and interaction parameters Ω are also given in the figure. As we can see, the interaction parameter Ω decreases from $Ag_xCu_{1-x}GaS_2$ to $Ag_xCu_{1-x}GaSe_2$ to $CuGa(S_xSe_{1-x})_2$ to $AgGa(S_xSe_{1-x})_2$, in the same order as lattice mismatch $\Delta a/\bar{a}$: 7.3%, 6.5%, 5.4%, 4.7%, respectively, indicating that strain is the dominating factor in determining the mixing enthalpies. These interaction parameters are relatively small, suggesting that the alloys can easily form at growth temperature.

V. CONCLUSION

In summary, we have calculated systematically the structural properties and electronic band structure of chalcopyrite compounds $AgGaS_2$, $AgGaSe_2$, $CuGaS_2$, $CuGaSe_2$, and their alloys, which could have important applications in solid state lighting and solar cells. We show that due to the increased structural and chemical freedom, these ternary compounds have some unusual physical properties. For example, the band gaps of $AgGaX_2$ are larger than the corresponding $CuGaX_2$ compounds, despite that the lattice constants of $AgGaX_2$ are much larger than for $CuGaX_2$. The valence band offsets between common-anion pairs $CuGaX_2/AgGaX_2$ are large and negative, whereas the valence band offsets between M^IGaS_2/M^IGaSe_2 are relatively small. The origin of these band structure anomalies are explained in terms of the atomic size difference between Cu and Ag and level repulsion between anion *p* and cation *d* orbitals. The band gap bowing parameters, bond lengths, and mixing enthalpies for the common-anion and common-cation alloys are also obtained and compared with available experimental results.

ACKNOWLEDGMENTS

The work at Fudan University was partially supported by the National Science Foundation of China, the Special Funds for Major State Basic Research, and the Shanghai Project. The computation was performed in the Supercomputer Center of Shanghai, the Supercomputer Center of Fudan University, and CCS. The work at NREL was funded by the U.S. Department of Energy, under Contract No. DE-AC36-99GO10337.

[1] J. L. Shay and J. H. Wernick, *Ternary Chalcopyrite Semiconductors: Growth, Electronic Properties and Applications* (Pergamon Press, Oxford, 1975).
[2] M. C. Ohmer, R. Randey, and B. H. Bairamov, Mater. Res. Bull. **23**, 16 (1998).
[3] R. W. Birkmire and E. Eser, Annu. Rev. Mater. Sci. **27**, 625 (1997).
[4] S. Chichibu, S. Shirakata, S. Isomura, and H. Nakanishi, Jpn. J. Appl. Phys., Part 1 **36**, 1703 (1997).
[5] S. N. Rashkeev and W. R. L. Lambrecht, Phys. Rev. B **63**, 165212 (2001).
[6] S. F. Chichibu, T. Ohmori, N. Shibata, T. Koyama, and T. Onuma, J. Phys. Chem. Solids **66**, 1868 (2005).
[7] T. J. Coutts, K. A. Emery, and J. S. Ward, Prog. Photovoltaics **10**, 195 (2002); T. J. Coutts, J. S. Ward, D. L. Young, K. A. Emery, T. A. Gessert, and R. Noufi, *ibid.* **11**, 359 (2003).
[8] A. Janotti and S.-H. Wei, Appl. Phys. Lett. **81**, 3957 (2002).
[9] I.-H. Choi and P. Y. Yu, Appl. Phys. Lett. **87**, 231909 (2005).
[10] *Semiconductors: Data Handbook*, 3rd ed., edited by O. Madelung (Springer, Berlin, 2004).
[11] D. J. Friedman and S. Kurtz, Prog. Photovoltaics **10**, 331 (2002).
[12] T. Tinoco, M. Quintero, and C. Rincon, Phys. Rev. B **44**, 1613 (1991).
[13] I.-H. Choi, S.-H. Eom, and P. Y. Yu, J. Appl. Phys. **87**, 3815 (2000).
[14] S. Park, S. K. Lee, J. Y. Lee, J.-E. Kim, H. Y. Park, H.-L. Park, H.-J. Lim, and W.-T. Kim, J. Phys.: Condens. Matter **4**, 579 (1992).
[15] J. L. Shay, B. Tell, H. M. Kasper, and L. M. Schiavone, Phys. Rev. B **5**, 5003 (1972).
[16] J. E. Jaffe and A. Zunger, Phys. Rev. B **28**, 5822 (1983).
[17] J. E. Jaffe and A. Zunger, Phys. Rev. B **29**, 1882 (1984).
[18] S.-H. Wei and A. Zunger, Phys. Rev. B **37**, 8958 (1988).
[19] S.-H. Wei and S. B. Zhang, J. Phys. Chem. Solids **66**, 1994 (2005).
[20] A. A. Lavrentiev, B. V. Gabrelýan, V. A. Dubeiko, and I. Y. Nikiforov, J. Struct. Chem. **42**, 385 (2001).
[21] S.-H. Wei, A. Zunger, I.-H. Choi, and P. Y. Yu, Phys. Rev. B **58**, R1710 (1998).
[22] G. Kresse and J. Furthmuller, Phys. Rev. B **54**, 11169 (1996).
[23] G. Kresse and J. Furthmuller, Comput. Mater. Sci. **6**, 15 (1996).
[24] J. P. Perdew, J. A. Chevary, S. H. Vosko, K. A. Jackson, M. R. Pederson, D. J. Singh, and C. Fiolhais, Phys. Rev. B **46**, 6671 (1992).
[25] P. E. Blochl, Phys. Rev. B **50**, 17953 (1994).
[26] G. Kresse and D. Joubert, Phys. Rev. B **59**, 1758 (1999).
[27] H. J. Monkhorst and J. D. Pack, Phys. Rev. B **13**, 5188 (1976).
[28] S. Froyen, Phys. Rev. B **39**, 3168 (1989).
[29] S.-H. Wei and A. Zunger, J. Appl. Phys. **78**, 3846 (1995).
[30] S.-H. Wei and A. Zunger, Appl. Phys. Lett. **72**, 2011 (1998).
[31] A. Zunger, S.-H. Wei, L. G. Ferreira, and J. E. Bernard, Phys. Rev. Lett. **65**, 353 (1990).
[32] S.-H. Wei, L. G. Ferreira, J. E. Bernard, and A. Zunger, Phys. Rev. B **42**, 9622 (1990).
[33] F. D. Murnaghan, Proc. Natl. Acad. Sci. U.S.A. **30**, 244 (1944).
[34] L. Garbato, F. Ledda, and R. Rucci, Prog. Cryst. Growth Charact. **15**, 1 (1987).
[35] H. Neumann, Phys. Status Solidi A **96**, K121 (1986).
[36] H. Neumann, Cryst. Res. Technol. **18**, 665 (1983).
[37] B. Fernandez and S. M. Wasim, Phys. Status Solidi A **122**, 235 (1990).
[38] M. H. Grimditch and G. D. Holah, Phys. Rev. B **12**, 4377 (1975).
[39] M. Bettini and W. B. Holzappel, Solid State Commun. **16**, 27 (1975).
[40] J. E. Rowe and J. L. Shay, Phys. Rev. B **3**, 451 (1971).
[41] S.-H. Wei and A. Zunger, Phys. Rev. B **49**, 14337 (1994).
[42] J. J. Hopfield, J. Phys. Chem. Solids **15**, 97 (1960).
[43] S. Laksari, A. Chahed, N. Abbouni, O. Benhelal, and B. Abbar, Comput. Mater. Sci. **38**, 223 (2006).
[44] A. Chalhed, O. Benhelal, S. Laksari, B. Abbar, B. Bouhafs, and N. Amrane, Physica B **367**, 142 (2005).
[45] S.-H. Wei, H. Krakauer, and M. Weinert, Phys. Rev. B **32**, 7792 (1985).
[46] L. Vegard, Z. Phys. **5**, 17 (1921).
[47] P. N. Keating, Phys. Rev. **145**, 637 (1966).
[48] J. L. Martins and A. Zunger, Phys. Rev. B **30**, 6217 (1984).
[49] S. Shirakata, A. Ogawa, S. Isomura, and T. Kariya, Jpn. J. Appl. Phys., Suppl. **32-3**, 94 (1993).